

Wavelet Transform Approach to High Impedance Fault Detection in MV Networks

Marek Michalik, Waldemar Rebizant, Mirosław Lukowicz
Institute of Electrical Power Engineering
Wrocław University of Technology, Poland

Seung-Jae Lee, Sang-Hee Kang
Next Generation Power Technology Center
Myongji University, Yongin, Korea

Abstract — Application of wavelet transform technique to high impedance arcing fault detection in distribution networks is presented. Phase displacement between discrete wavelet coefficients calculated for zero sequence voltage and current signals at natural network frequency is tracked. The developed wavelet based HIF detector has been tested with EMTP-ATP generated signals, proving better performance than traditionally used algorithms and methods. The protection method proposed is efficient, robust and may be used for HIF detection independently of the network neutral point grounding mode.

Index Terms — protective relaying, wavelet transform, distribution networks, high impedance arcing faults, transient analysis.

I. INTRODUCTION

DETECTION of high impedance faults (HIFs) presents still important and unsolved protection problem, especially in distribution networks. Discrimination of the feeder with arcing ground connection is not trivial since the ground fault current in MV networks is very low, often below load current of the feeder. Several approaches for the detection of HIFs may be found in the literature, applying algorithms monitoring:

- low frequency spectrum of the current [4],
- incremental variance of even order harmonic power [3],
- energy variations in a concerned frequency band [6],
- wavelet coefficients of the line currents [1], etc.

In this paper the idea of detecting HIFs by comparing phase angles of CWT coefficients, suggested previously in [1] as a possible technique for transmission line level, is thoroughly studied. Its new version expanded for MV networks is presented and the results of its extensive simulative testing are described.

The following sections of the paper describe the arc model developed and its application in modeling of MV network events (Sec. II), basic information on the wavelet technique and the HIF detection algorithm itself (Sec. III) as well as scheme testing with various ATP-generated signals (Sec. IV). Conclusions close the paper.

II. ARC MODEL AND SIMULATIONS PERFORMED

A. The arc model adopted

The high impedance ground fault model applied in simulation experiments was developed basing on research and considerations presented in [3, 4, 9] but some new features were also included into the model implementation. To obtain dynamic features of the ground fault nonlinear impedance the

digital arc model described in [9] was adopted. This model is derived from Hochrainer arc description that is based on energy balance in the arc and is described by the following differential equation:

$$\frac{dg(t)}{dt} = \frac{1}{T} (G(t) - g(t)) \quad (1)$$

that is equivalent to the transfer function

$$\frac{g(s)}{G(s)} = \frac{1}{Ts + 1} \quad (2)$$

where: $g(t)$ – time-varying arc conductance, $G(t)$ – stationary arc conductance, T – time constant and $r(t)=1/g(t)$ is time-varying arc resistance.

The stationary arc conductance follows as

$$G(t) = \frac{|i(t)|}{(u_p + R|i(t)|)l_p} \quad (3)$$

where: $i(t)$ – arc current, u_p – constant voltage parameter per arc length, R – resistive component per arc length ($R=9 \Omega/\text{cm}$), l_p – arc length ($l_p=10 \text{ cm}$).

The length of the arc l_p as well as the time constant T were considered to be constant in the investigations.

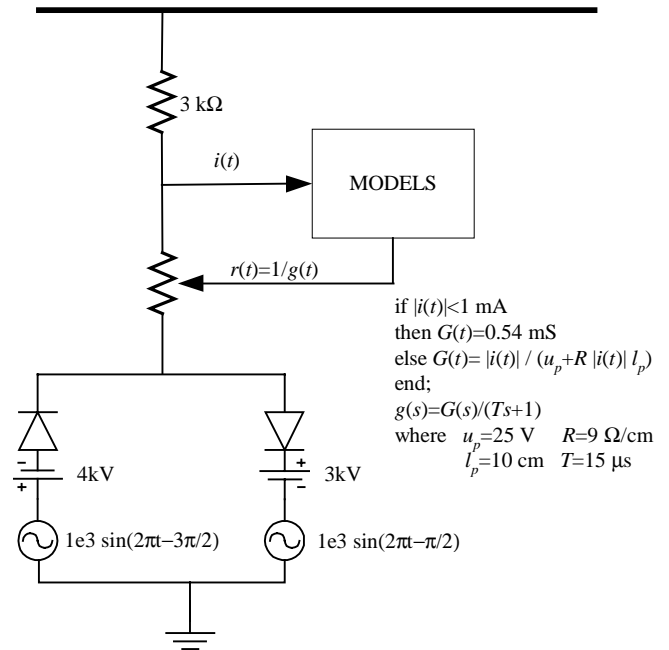


Fig. 1. Arc model structure.

The developed arc model was implemented using the ATP facilities and the MODELS in particular (Fig. 1). Diodes and polarizing ramp voltages were used to control arc ignition instants. The arc model consists of the linear resistor (representing the ground path resistance), the nonlinear time-varying resistor $r(t)$ (representing the dynamic arc) as well as DC and AC sources. The sources ensure asymmetry of the arc current and voltage (DC sources) and variable arc ignition and quenching point (AC sources). The onset arc voltages V_p , V_N ($V_p=3\text{kV}$ and $V_N=4\text{kV}$) were applied that were supplemented with additional AC sources of 1 kV magnitude and very low frequency. The resulting v - i characteristic of the arc and variable arc resistance are shown in Fig. 2. The characteristic corresponds fairly to the experimental results presented in [4]. The high impedance model was switched into the modeled MV network at points of fault inception.

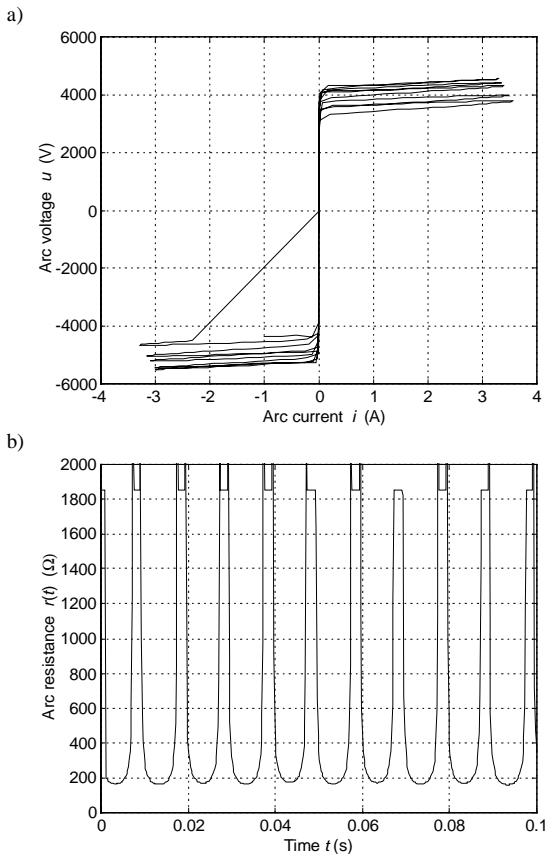


Fig. 2. v - i characteristic of the arc modeled (a) and its variable resistance (b).

B. MV network model and HIF simulation results

In Fig. 3 the MV (15kV) network analyzed in ATP program is presented. The network under consideration is an example of a typical real Polish distribution network. It is supplied from the 110 kV system (short-circuit power 1672 MVA) via a step-down transformer T1 (16 MVA, Yd11, 110/15 kV). The network is of a mixed type, i.e. it consists of both overhead lines and cables. The network may be operated in isolated, compensated or resistively earthed mode. The network grounding is done via an additional earthing transformer T2 (865 kVA, Zy11). The total capacitive current of the network is 56 A.

Using the ATP program single-phase earth faults were simulated at point F1 (at the end of line L_1). Below a few examples of network operation under faulty conditions are shown. The high-ohmic arc model developed was included in all cases. The $3U_0$ voltage and $3I_0$ current in the faulty line (secondary signals) for the isolated neutral point are shown in Fig. 4. In this case, due to directional properties of the arc, the high and slowly decaying DC component appears in the zero sequence voltage $3U_0$. The $3I_0$ remains symmetrical. The $3I_0$ and $3U_0$ signals for the network with compensation (Petersen coil) are shown in Fig. 5.

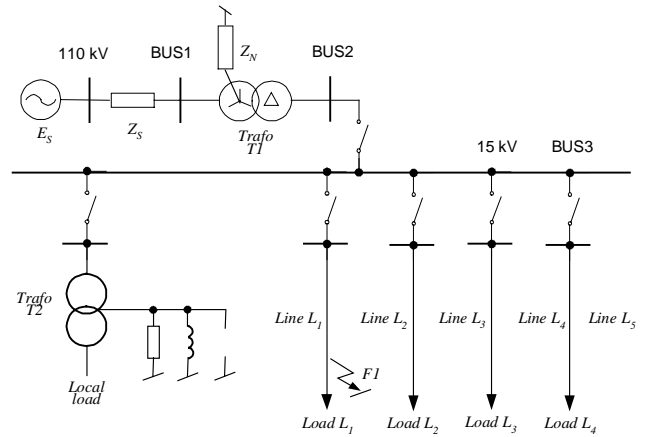


Fig. 3. MV network studied.

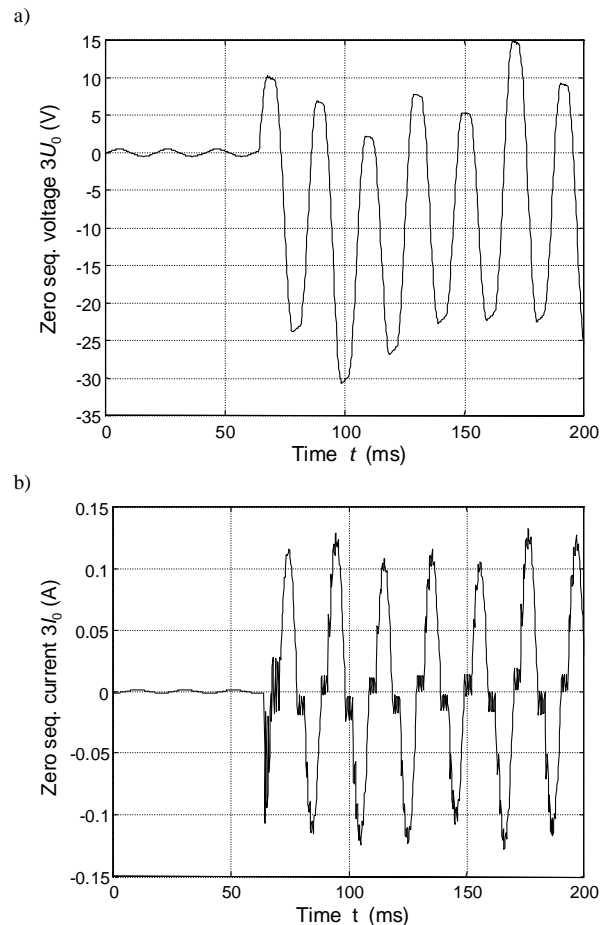


Fig. 4. Example of $3U_0$ (a) and $3I_0$ (b) for the high-ohmic ground fault at the end of a cable line for the isolated network neutral point.

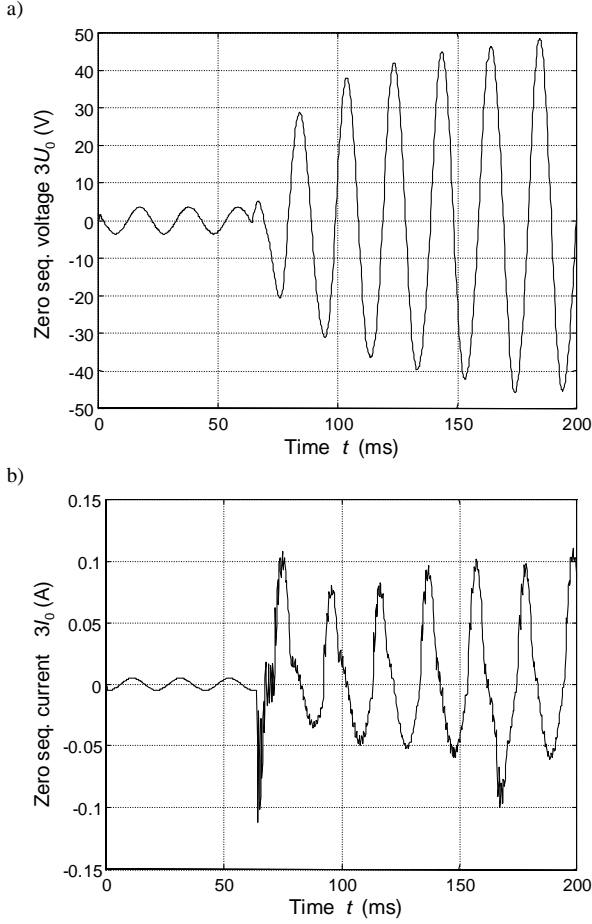


Fig. 5. Example of $3U_0$ (a) and $3I_0$ (b) for the high-ohmic ground fault at the end of a cable line for the compensated MV network.

III. WAVELET BASED HIF DETECTION

A. Principle of the method

The ground fault detection algorithm developed is based on analysis of higher frequency transient components of the zero sequence ground fault current and voltage. Analysis is carried out by use of wavelet transform.

The wavelet analysis uses specific approximation functions that are called mother wavelets. By definition, a continuous wavelet transform (CWT) of the continuous signal $x(t)$ for the mother wavelet function $g(t)$ is defined as [5]:

$$CWT(a, b) = \frac{1}{\sqrt{a}} \int_{-\infty}^{\infty} x(t) g\left(\frac{t-b}{a}\right) dt \quad (4)$$

where a and b are the continuous coefficients of scale (dilatation) and translation, respectively. The former sets the time duration of the wavelet while the latter changes the wavelet position in time domain. In this paper the complex Morlet mother wavelet of the form

$$g(t) = e^{-\frac{\pi^2}{2}} e^{j2\pi t} \quad (5)$$

was applied to determine the wavelet coefficient of the signals analyzed for baby wavelet corresponding to given frequency (f_n). Out of two complex conjugate components of (5) the ‘active’ one

was used that, after substitution to (4) and representation in discrete form, yields

$$CWC(a, b) = \frac{1}{\sqrt{a}} \sum_{n=0}^{N-1} x(k-n) g\left(\frac{n-b}{a}\right) \quad (6)$$

where $x(k)$ is $3I_0(k)$ or $3U_0(k)$, respectively, and

$$g\left(\frac{n-b}{a}\right) = e^{-\pi \frac{(n-b)^2}{a^2}} \cos \frac{2\pi(n-b)}{a} \quad (7)$$

The CWC coefficient (baby wavelet) for signal $x(k)$ of frequency f_n at specified sampling frequency f_s is obtained when $a=f_s/f_n$, $b=\pi a/2$ and $N=2b$, with data window length N rounded up to the nearest even integer. The example of wavelet $g(k, a, b)$ calculated from (7) is shown in Fig. 6.

For ground fault detection the CWC wavelet coefficients were calculated with wavelet $g(k, a, b)$ tuned to the natural frequency f_n of transient damped components of the MV network that are always present in $3U_0(k)$ and $3I_0(k)$ during a fault. This frequency is specific for the network protected (it usually lies in the frequency range 150–850Hz, i.e. 3rd–17th harmonic, depending on the network size and configuration) and can be estimated from the equation

$$f_n = \frac{1}{2\pi \sqrt{3L_s(C_0 + C_p)}} \quad (8)$$

where: L_s – the supplying source inductance, C_0 – the network total phase-to-ground capacitance, C_p – the network total phase-to-phase capacitance.

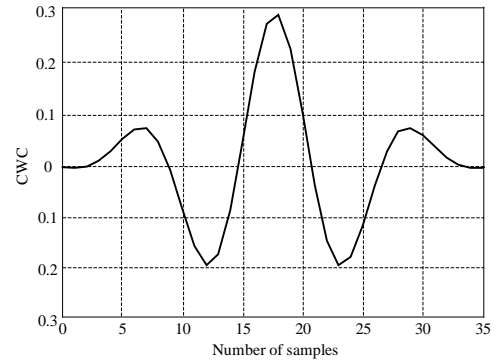


Fig. 6. Example of Morlet wavelet (5) calculated for $a=12$, $b=18$ and $N=36$.

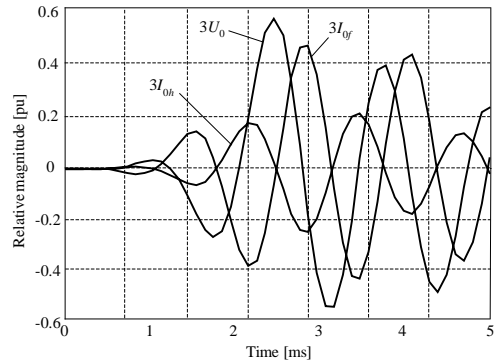


Fig. 7. Example of wavelet coefficient phase relation for $3U_0$, $3I_{of}$ (faulty phase) and $3I_{oh}$ (healthy phase); ground fault in isolated network at the end of 5km overhead line, $f_n=750\text{Hz}$, $f_s=5\text{kHz}$.

The idea of the HIF detection algorithm is based on determination of phase displacement relation between wavelet coefficients of $3U_0(k)$ and $3I_0(k)$. Observation of transients in $3I_0(k)$ shows that during ground fault any $3I_0$ current component of the same frequency in faulty line and in healthy ones is in opposition while the phase displacement of the corresponding transient components of zero sequence voltage $3U_0$ is located in between of the current component waveforms and never exceeds $-\pi/2$ in faulty line and $+\pi/2$ in healthy one. This feature projects to the corresponding wavelet coefficients phase relation as it is illustrated in Fig. 7. The figure shows the wavelet coefficients waveforms obtained for transient component of frequency $f_n=750$ Hz from $3U_0$ and $3I_0$ in faulty and healthy line for the ground fault in isolated MV network. The estimation of phase displacement between voltage and current wavelet coefficients for the time instant at which the voltage coefficient reaches maximum peak value can be used for effective determination whether the ground fault is located inside or outside of the protected line.

B. Decision-making scheme

Broader time range of HIF detection algorithm operation is shown in Fig. 8. It is visible that the algorithm issues numerous subdecision signals every 10 ms, i.e. at each consecutive arc ignition. It can also be seen that among the majority of correct bursts (9 out of 11 peaks within the presented period of time) some incorrect indications on the fault in the healthy line may occur due to some transient errors. To overcome this problem the final decision related to faulted feeder identification is to be taken after the detection peaks of one type (issued for given feeder) are repeated at least preset number of times. Another decision-making approaches based on multicriterial analysis (with use of other criterion signals) or fuzzy logic may also be considered to improve the scheme operation.

The decision-making scheme adopted for HIF detection is described in this section. The scheme, which can be called the integrating one, is based on simple principle of counting events that are generated in the process of phase displacement measurement between CWCs of $3U_0$ ($CWC_{U_0}(k)$) and $3I_0$ ($CWC_{I_0}(k)$) in the protected feeder.

The basic algorithm flow chart is shown in Fig. 9. The idea of the algorithm operation is based on measurement of the phase displacement between $CWC_{U_0}(k)$ and $CWC_{I_0}(k)$ at the instant of time for which the $|CWC_{U_0}(k)|$ waveform reaches the local maximum peak value $D_{U_{max}}$. At this specific time instant the signs $SGNU$ and $SGNI$ of $dCWC_{U_0}(k)$ and $dCWC_{I_0}(k)$ derivatives are determined and compared:

$$SGNU = \text{sgn}[dCWC_{U_0}(k)] = \text{sgn}[CWC_{U_0}(k_{max}) - CWC_{U_0}(k_{max}-1)] \quad (9)$$

$$SGNI = \text{sgn}[dCWC_{I_0}(k)] = \text{sgn}[CWC_{I_0}(k_{max}) - CWC_{I_0}(k_{max}-1)] \quad (10)$$

If the signs are the same the line is detected as faulty (see Fig. 8), otherwise the line is healthy and event is not generated. The final decision, however, is taken and the positive event is generated when the $D_{U_{max}}$ value is greater than the

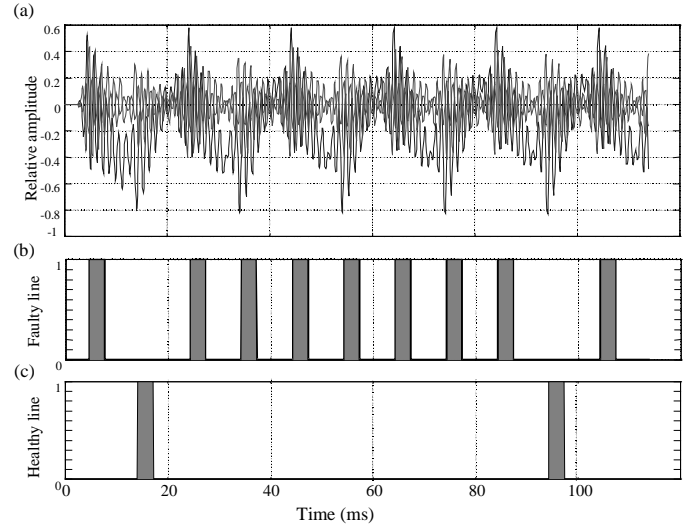


Fig. 8. Operation of the proposed HIF detection algorithm for a fault in the network with isolated neutral point: a) CWCs for the zero sequence signals as in Fig. 5, b) indication on the faulty line, c) indication on the healthy line.

preset value of the decision-activating threshold DAT . The value of this threshold should be set at the level that exceeds 2-4 times the level of the background harmonic noise that is always present in the network normal operating conditions, in particular, when the nonlinear loads are supplied. The flag A (see Fig. 9) is used to determine whether the part of the $CWC_{U_0}(k)$ waveform of the positive ($A=1$) or of the negative ($A=0$) slope is being processed.

Each positive event increases the event counter state by one. The first positive event starts the timer procedure that generates preset delay time period τ . If at the end of τ the number of counted events exceeds the preset value M_{CR} an alarm is triggered on and the counter is set to zero. Assuming that minimum 2 events are generated in one half-cycle of the fundamental frequency f_1 (arc ignition and extinction) the value of M_{CR} can be determined by simple formula:

$$M_{CR} = 4 \tau f_1 \quad (11)$$

In the experiments the M_{CR} was equal to 20 (for $\tau=0.1s$).

IV. ALGORITHM TESTING

Numerous testing scenarios have been prepared and tests carried out to investigate the HIF detecting algorithm performance. EMTP signals from high impedance faults at various points of overhead and cable feeders were gathered. The algorithms' robustness for transients associated with switching operations in the network including line energizing and de-energizing and capacitor bank switching were also examined.

A. High impedance ground faults on feeders - unbroken and broken conductor

In all tests the HIF detection algorithm proved to be selective and reliable. Very rare missing alarms on faulty lines and no inadvertent alarms on healthy feeder were observed. The example of the integrating algorithm operation is shown in Fig. 10. The enlarged CWC waveforms from Fig. 10 are similar to those shown in Fig. 7.

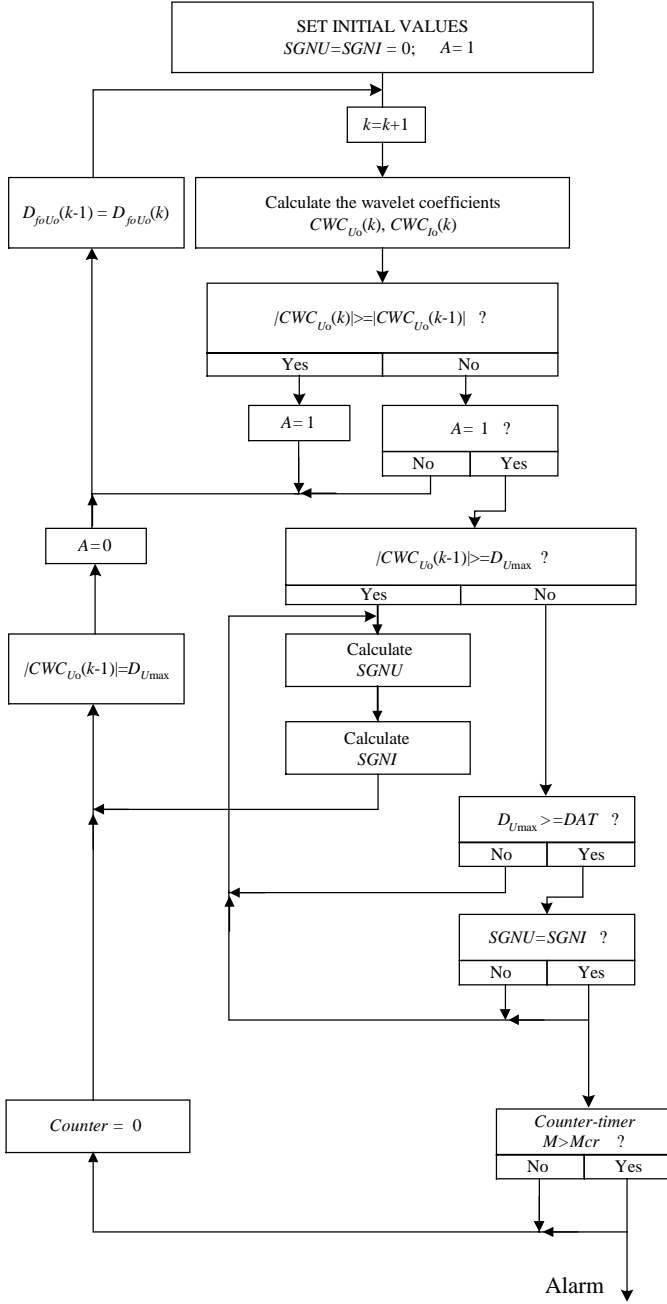


Fig. 9. Flow chart of the integrating decision-making algorithm.

The rare spurious positive events appear on healthy feeders (Fig. 10c) when the trailing edge of a decaying *CWC* waveform is at the brink of the neutral current background noise level. It was noticed during the tests that the most difficult conditions for ground fault detection appear in the compensated network due to the presence of Petersen coil that significantly reduces the value of the ground fault current. As a result the arc becomes intermittent [4] decreasing the number of positive events counted in preset period. The problem can be solved by reduction of the alarm triggering level. During the experiments on compensated network reduction of alarm triggering level by half ($M_{CR}=10$) practically eliminated missing alarm trippings for remote faults.

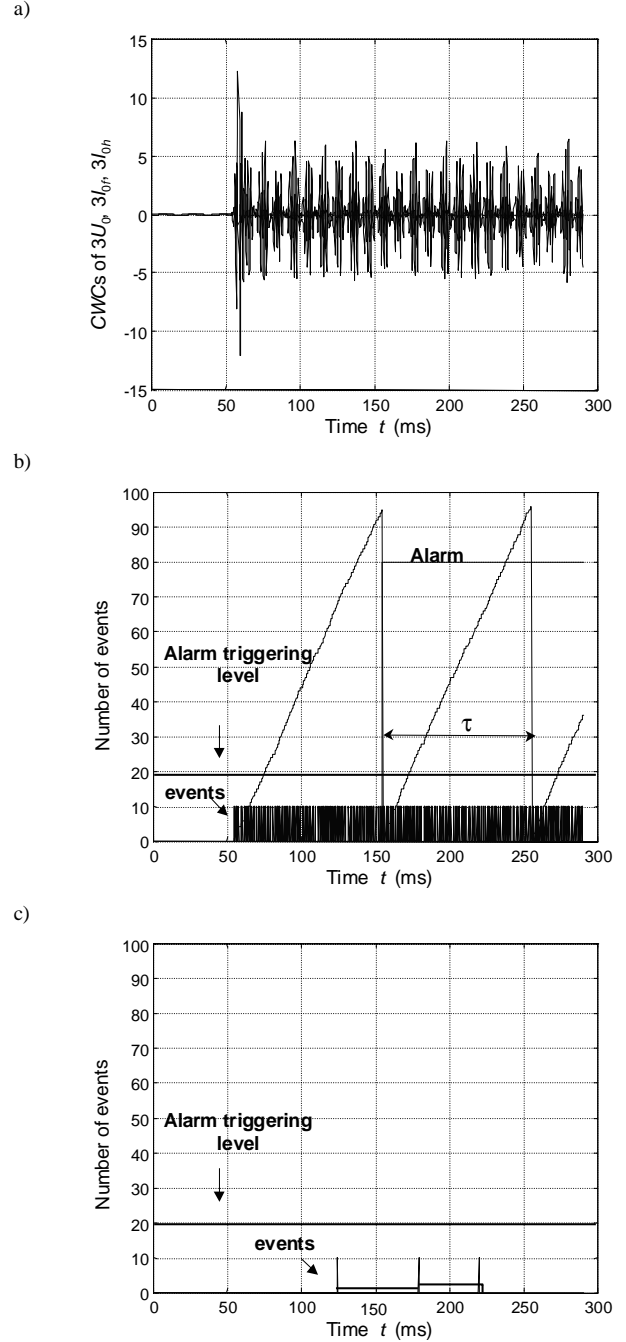


Fig. 10. Detection of a high impedance ground fault by use of the integrating algorithm; compensated network, fault at the end of 20 km overhead feeder; (a) - *CWCs* of $3U_0$, $3I_{of}$ (faulty line) and $3I_{oh}$ (healthy line); algorithm performance in faulty feeder (b) and in healthy feeders (c).

B. Energizing and de-energizing of a feeder

If a feeder is energized or de-energized the source of higher harmonic associated with switching the transients on the circuit breaker is located inside protected zone and may be detected as high impedance fault. This case is illustrated in Fig. 11. However, the short train of positive events (see Fig. 11b) seen practically when the feeder is de-energized (1–5 events) was not long enough to trigger alarm in switched feeder. More important is that due to directional property of the method there is no attempt to trigger alarm in remaining loaded feeders.

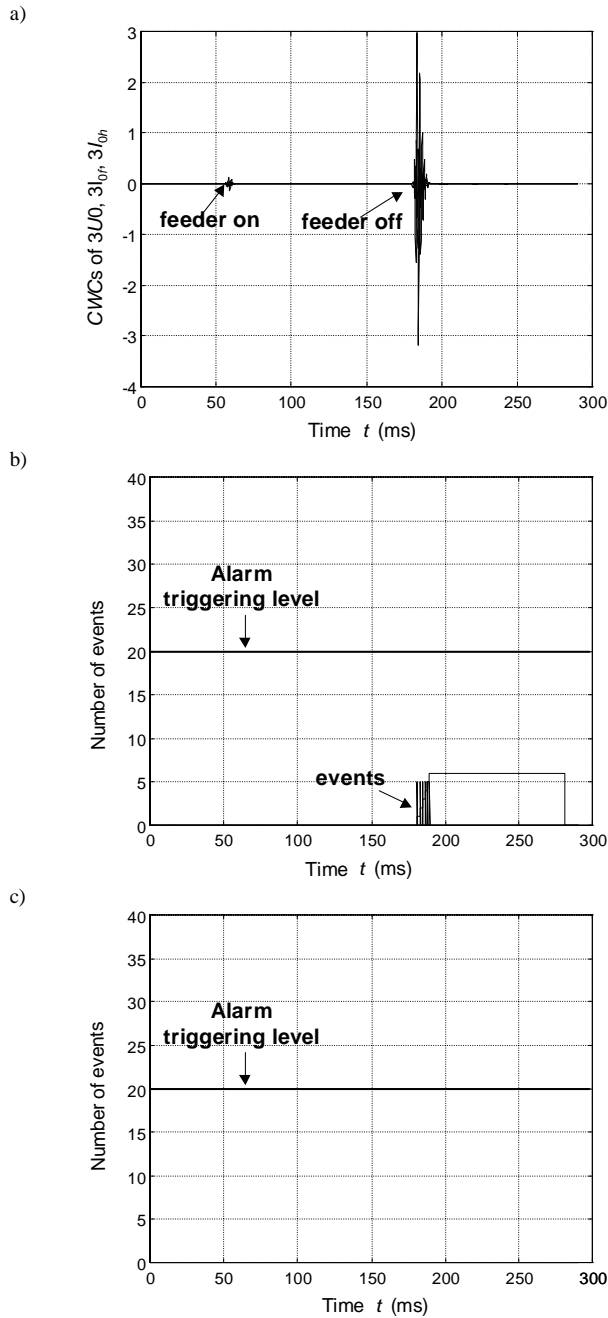


Fig.14. Energizing and de-energizing of a feeder in the compensated network; CWCs of $3U_0$, $3I_{0f}$ in energized and de-energized feeder (a), algorithm performance in the energized and de-energized feeder (b) and in other lines (c).

V. CONCLUSIONS

In the paper the application of discrete form of the Continuous Wavelet Transform to detection of high impedance ground faults in distribution MV networks is presented. The ground faults are detected by estimation of phase displacements between CWCs of zero sequence voltage $3U_0$ and $3I_{0f}$ currents in the feeders. It is shown that analyses of transients in zero sequence currents and voltages in wavelet domain lead to fast and reliable HIF detection and localization of the faulted feeder. The algorithm responds properly to high impedance arcing faults and remains stable for other fast

changes in the network, independently of the network neutral point grounding mode.

The HIF detection technique with application of wavelet coefficients is supported with additional logic scheme. The algorithm sub-decision signals are additionally integrated. The final decision related to faulted feeder identification is taken after the detection peaks of one type (issued for given feeder) are repeated at least preset number of times. It is shown that such an approach leads to reliable decisions concerning state of the protected feeders, with no malfunctions for other non-fault transients in the network.

The algorithm of high impedance arcing fault detection has been tested with EMTP-ATP generated signals. Various situations of faults within and outside of the protected line as well as other cases of normal operation (e.g. capacitor bank switching) were simulated. Numerous examples proved perfect operation of the developed algorithm under various transient conditions in MV network.

VI. ACKNOWLEDGEMENTS

The authors would like to thank Korea Ministry of Science and Technology and Korea Science and Engineering Foundation for their support through ERC program. A part of financial support for the research conducted was also gratefully received from the Ministry of Science and Information Society Technologies of the Republic of Poland.

VII. REFERENCES

- [1] O. Chaari, M. Meunier and F.Brouaye: "Wavelets: A new tool for the resonant grounded power distribution systems relaying", *IEEE Transactions on Power System Delivery*, Vol. 11, No. 3, July 1996, pp. 1301-1038.
- [2] H. Magnago and A. Abur: *Fault location using wavelets*, *IEEE Transactions on Power System Delivery*, Vol. 13, No. 4, October 1998, pp. 1475-1480.
- [3] D.C.T. Wai and X. Yibin: "A Novel Technique for High Impedance Fault Identification", *IEEE Transactions on Power Delivery*, Vol. 13, No. 3, July 1998, pp. 738-744.
- [4] A.E. Emanuel and E.M. Gulachenski: "High Impedance Fault Arcing on Sandy Soil in 15kV Distribution Feeders: Contribution to the Evaluation of the Low Frequency Spectrum", *IEEE Trans. on Power Delivery*, Vol. 5, No. 2, April 1990, pp. 676 – 686.
- [5] W.H. Kwon, G.W. Lee, Y.M. Park, M.C. Yoon and M.H. Yoo: "High Impedance Fault Detection Utilizing Incremental Variance of Normalized Even Order Harmonic Power", *IEEE Trans. on Power Delivery*, Vol. 6, No. 2, April 1991.
- [6] C.-J. Kim and B.D. Russel: "Harmonic Behaviour during Arcing Faults on Power Distribution Feeders", *Electric Power System Research*, Vol. 14, 1988, pp. 219-225.
- [7] X. Yibin, D.C.T. Wai and W.W.L. Keetherpala: "A New Technique Using Wavelet Analysis for Fault Location", *Proc. of DPSP'97 Conference*, IEE, UK, March, 1997, pp. 231-234.
- [8] H. Kim and R.K. Aggarwal: "Wavelet transforms in power systems, part 1 – General introduction to the wavelet transform", *Power Engineering Journal* 2000.
- [9] M.Kizilcay and T. Pniok: "Digital System Simulation of Fault Arcs in Power Systems", *ETEP*, Vol. 1, No. 1, January/February 1991, pp. 55-60.

VIII. BIOGRAPHIES



Marek Michalik - received the M.Sc. degree in Electronics from the Technical University of Wrocław, Poland in 1968. He was first with the Institute of Power Systems. In 1969 he joined the Electrical Engineering Dept. of Wrocław University of Technology from which he received his PhD degree in 1975. He is still with WUT as the assistant professor. His research interests are: digital signal processing for power system relaying and microprocessor system application to power system control. (marek.michalik@pwr.wroc.pl).



Waldemar Rebizant (M'2000) was born in 1966 in Wrocław, Poland. He received his M.Sc., Ph.D. (both with honors) as well as D.Sc. degrees from Wrocław University of Technology, Poland in 1991 and 1995, respectively. Since 1991 he has been a faculty member of Electrical Engineering Faculty at the WUT. In June 1996 he was awarded Siemens Promotion Prize for the best dissertation in electrical engineering in Poland in 1995. In 1999 he was granted a prestigious Humboldt research scholarship for the academic year 1999/2000. In the scope of his research interests are: digital signal processing and artificial intelligence for power system protection purposes. (waldemar.rebizant@pwr.wroc.pl)



Mirosław Łukowicz was born in 1969 in Poland. He received M. Sc. and Ph.D. degrees from the Wrocław University of Technology, Poland in 1993 and 1998, respectively. He is now an assistant professor at the Institute of Electrical Power Engineering at Wrocław University of Technology. His research activities are modeling and analyzing of transient phenomena in power systems, application of AI techniques to signal processing and decision-making in protective relaying. (miroslaw.lukowicz@pwr.wroc.pl)



Seung-Jae Lee (S'1978, M'1988) was born in Seoul, Korea in 1955. He received BS and MS degrees from Seoul National University, Korea in 1979 and 1981, respectively and Ph.D. from University of Washington, Seattle, USA in 1988. Since 1988 he has been with the Department of electrical Engineering, Myongji University as a Professor. He is also a director of Next Generation Power Technology Center. His main research areas are protective relaying, distribution automation and AI applications to power systems. (sjlee@mju.ac.kr)



Sang-Hee Kang (S'1990, M'1993) is an associate professor at Myongji University, Korea. He received the BS, MS and Ph.D. degrees from Seoul National University, Korea in 1985, 1987 and 1993, respectively. He was a visiting fellow and a visiting scholar at the University of Bath, UK in 1991 and 1999. His research interest is to develop digital protection systems for power systems using digital signal processing techniques. (shkang@mju.ac.kr)